HHS Public Access

Author manuscript

*Hear Res*. Author manuscript; available in PMC 2017 March 01.

Published in final edited form as:

*Hear Res*. 2016 March ; 333: 225–234. doi:10.1016/j.heares.2015.08.018.

# Delayed loss of hearing after hearing preservation cochlear implantation: human temporal bone pathology and implications for etiology

**Alicia M. Quesnel**[a], **Hideko Heidi Nakajima**[a], **John J. Rosowski**[a], **Marlan R. Hansen**[b], **Bruce J. Gantz**[b], and **Joseph B. Nadol Jr.**[a]

Alicia M. Quesnel: alicia_quesnel@meei.harvard.edu; Hideko Heidi Nakajima: heidi_nakajima@meei.harvard.edu; John J. Rosowski: john_rosowski@meei.harvard.edu; Marlan R. Hansen: marlan-hansen@uiowa.edu; Bruce J. Gantz: bruce-gantz@uiowa.edu; Joseph B. Nadol: joseph_nadol@meei.harvard.edu

[a]Department of Otology and Laryngology, Harvard Medical School, Massachusetts Eye and Ear Infirmary, 243 Charles Street, Boston, Massachusetts 02114 USA

[b]University of Iowa Hospitals and Clinics, Department of Otolaryngology, 200 Hawkins Drive, Iowa City, Iowa 52242-1078 USA

## Graphical Abstract

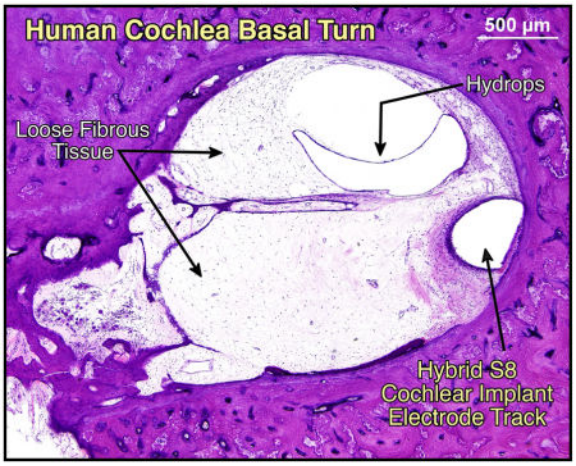


## 1. Introduction

The cochlear implant is a highly successful neural prosthesis, which restores or improves speech understanding in patients with severe to profound sensorineural hearing loss. Over the past three decades, the criteria for cochlear implant candidacy have expanded considerably due to improvements in both cochlear implant performance and the ability to

Correspondence to: Alicia M. Quesnel, MD, Massachusetts Eye and Ear Infirmary, 243 Charles Street, Boston, MA 02114, Tel (617) 573-3503, Fax (617) 573-3939, alicia_quesnel@meei.harvard.edu.

preserve residual hearing with cochlear implantation. On March 20 2014, the United States Food and Drug Administration approved the Nucleus® Hybrid™ L24 Cochlear Implant System (Cochlear Limited, New South Wales, Australia) for patients with severe to profound high frequency sensorineural hearing loss, yet normal to moderately impaired low frequency hearing (www.fda.gov). After multiple clinical trials demonstrating the feasibility of hearing preservation and benefits of shorter electrodes intended for combined electric and acoustic stimulation(Gantz & Turner 2004; Gantz et al. 2009; Lenarz et al. 2013), cochlear implantation for patients with significant residual low frequency hearing has transitioned from an investigational procedure to routine care.

Initial preservation of residual hearing after cochlear implantation can be achieved to varying degrees in 50% to 100% of cases (Lenarz et al. 2013; Adunka et al. 2013; Huarte & Roland 2014; Usami et al. 2014; Gstoettner et al. 2009). When residual hearing is preserved, patients may utilize both electric and acoustic hearing in the implanted ear. The benefits of combined electric and acoustic hearing in the same ear include better hearing in background noise and in quiet, and better spatial localization (Reiss, Turner, Karsten, Erenberg, Taylor & Gantz 2012a; Gantz et al. 2009; Turner et al. 2008; Gantz & Turner 2004; Gifford et al. 2014; Kiefer et al. 2005). These benefits occur when the preserved hearing is in the functional acoustic range (less than 90 dB pure tone average for 125Hz to 1.5KHz) (Roland et al. submitted 2015). Furthermore, preservation of low frequency hearing is important for music appreciation in patients with electric-acoustic implants (Golub et al. 2012).

While many patients with preserved hearing after implantation maintain that hearing level, a subset of these patients experience progressive hearing loss over the months following cochlear implantation. Delayed post-implantation hearing loss has been reported in 15 to 56% of patients with initially preserved hearing (Gifford et al. 2013; Reiss, Turner, Karsten, Erenberg, Taylor & Gantz 2012b; Van Abel et al. 2015; Lenarz et al. 2013; Adunka et al. 2013). In the Hybrid 10 clinical trial, for example, although only 2 out of 87 patients were found to have total hearing loss at the initial one month follow up, an additional 6 patients progressed to total hearing loss between 3 and 24 months after implantation(Gantz et al. 2009). Furthermore, between 3 to 12 months after implantation, hearing loss progressed more than 30 decibels in 25% of the patients(Gantz et al. 2009).

The etiology of this delayed hearing loss after implantation is not well understood. Possible etiologies include (1) inflammatory cascade(O'Leary et al. 2013) and immunogenic response(Nadol et al. 2008), (2) excitotoxicity from electrical stimulation (Kopelovich et al. in press 2015), (3)delayed degeneration of hair cells (Eshraghi et al. 2007), spiral ganglion neurons, or their synapses, (4) delayed effects of trauma to intracochlear structures such as the stria vascularis or spiral ligament, (5) progressive alterations in cochlear mechanics due to intracochlear fibrosis and/or new bone formation, or other disease processes such as intracochlear otosclerosis, and (6) post-implantation conductive hearing loss (Chole et al. 2014). Understanding the etiology of delayed post implantation hearing loss is critical for guiding both clinical management of cochlear implant patients with significant residual hearing and future research directed toward improving hearing preservation with cochlear implantation.

Here we present the human temporal bone pathology from a patient implanted during life with the Iowa/Nucleus Hybrid S8 cochlear implant, who had delayed loss of initially preserved hearing after implantation. Multiple potential mechanisms of the delayed loss of residual hearing based on the histopathologic findings and cochlear mechanics are discussed.

## 2. Materials and Methods

### 2.1 Case report

This 70 year old man had slowly progressive, high frequency sensorineural hearing loss that was first diagnosed at approximately 30 years of age. As a factory worker, he had occupational noise exposure for many years. He also had two brothers with hearing loss of unknown etiology and unknown age of onset. The etiology of his hearing loss was presumably related to genetic predisposition and noise exposure.

He was fitted with binaural amplification at age 42. He had progressive hearing loss, and underwent a cochlear implant evaluation because of limited benefit from his binaural amplification (Figure 1A, Table 1). At age 63, he underwent cochlear implantation of the left ear with the Iowa/Nucleus Hybrid S8 electrode Freedom cochlear implant (Cochlear Americas, CO, USA). The Hybrid S8 electrode array is 10 mm in length with 6 channels distributed over the distal 4.3 mm (Figure 2). A canal wall up mastoidectomy with facial recess approach was used, and a 0.5 mm cochleostomy was drilled anterior and inferior to the round window. A “soft surgical technique” was employed; this included reduced drill speed, atraumatic opening of the cochlear endosteum with a microinstrument (rather than entry into the cochlea with the drill), avoidance of suctioning once the scala tympani was opened, and slow insertion of the electrode. All 6 electrode contacts were fully inserted, and the cochleostomy was sealed with fascia.

An initial post-operative audiogram at 4 weeks after implantation demonstrated preservation of residual low frequency hearing at a level of moderate to severe hearing loss (Figure 1B). A follow up audiogram at 18 weeks after implantation identified progression of left sided hearing loss to a profound level (Figure 1C). The patient did not report a sudden decrement in his hearing or cochlear implant performance. He was treated with oral prednisone, but the left sided hearing loss did not recover (Figure 1D).

Of note, he did not receive excessive electrical stimulation of his cochlear implant. Levels of stimulation for his cochlear implant between 4 to 18 weeks were similar, for example, to levels typically programmed for Nucleus® Contour Advance™ implantees (Cochlear Ltd., Australia) (Figure 3A). The impedances of the 6 electrodes in his S8 cochlear implant did not increase over time (Figure 3B). At 6 months, the impedances for electrodes 4 and 5 decreased (Figure 3B). This correlated with the general timing of hearing loss, however, the reason for the decrease in impedances in these electrodes is not clear.

At 4 years post-implantation, the performance as measured by CNC word recognition was 28% for the left CI alone and 73% in the bimodal condition (left ear with electric stimulation via cochlear implant and right ear with hearing aid) (Table 1). Since he had significant

benefit in the bimodal condition, he continued to wear his left cochlear implant (with electric stimulation only) and right hearing aid.

The patient passed away 7 years after cochlear implantation due to complications of bladder cancer.

### 2.2 Histologic preparation

Both temporal bones were removed at 35 hours after death, and fixed in formalin. High resolution temporal bone protocol thin slice (0.5mm collimation) multidetector computed tomography (CT) imaging was performed on the specimens. The cochlear implant electrode was removed from the implanted left temporal bone. The specimens were then decalcified in ethylenediamine tetra-acetic acid, dehydrated in graded alcohols, embedded in celloidin, and serially sectioned in the axial plane at a thickness of 20 um. Every 10th section was stained with Hematoxylin and Eosin and mounted on a glass slide for histologic examination(Merchant SN 2010).

A 2 dimensional (2D) reconstruction of each cochlea was performed(Merchant SN 2010). In this method, tangential sections at the level of the inner and outer pillar cells are used to calculate the cochlear duct length. Cell counts of inner hair cells, outer hair cells, and spiral ganglion neurons were performed for each stained slide containing these cells according to previously established methods. The presence of soft tissue fibrosis, new bone formation, and the location of the electrode was marked on the 2D reconstruction after examining each stained slide through the cochlea. A 3 dimensional (3D) reconstruction of the cochlea from the CT images was used to determine the intracochlear electrode length(O'Malley et al. 2014).

## 3. Results

### 3.1 Computed Tomography (CT)

Post mortem CT of the implanted (left) temporal bone showed the electrode array to be positioned along the lateral wall in the basal turn of the scala tympani (Figure 4). The measured intracochlear array length was 6.5mm on the 3D reconstruction created from the CT images.

### 3.2 Temporal Bone Histopathology

The unimplanted right ear and implanted left ear cochlear ducts measured 32.9mm and 33.3mm in length on 2D reconstruction, respectively. In both ears, the inner and outer hair cells were totally missing in the basal 18 mm of the cochleae. Apically in both ears, scattered loss of inner hair cells and moderate to severe loss of outer hair cells was observed. Patchy mild to moderate degeneration of the stria vascularis and mild degeneration of the spiral ligament was found throughout the cochleae on both sides (Figures 5 and 6). In the implanted left ear, hydrops, i.e. distension of Reissner's membrane, was noted throughout the basal half of the basal turn up to 2.4 mm beyond the tip of the electrode (i.e. up to millimeter 11.8) (Figure 6).

The spiral ganglion neuron cell counts were similarly reduced in both ears (Table 2), with 44% loss in the right ear and 49% loss in the left ear when compared to normal for age. Visual inspection of dendritic process density within the osseous spiral laminae, without quantification, did not reveal any appreciable differences in the left ear compared to the right. The semicircular canals, utricle and saccule were normal bilaterally, with the exception of an area of atrophy of the saccular neuroepithelium in the implanted left ear.

In the left ear, the cochleostomy was located at millimeter 5 from the basal end of the cochlea and was 0.65 mm in diameter in the axial plane. The electrode array track began at millimeter 5 in the scala tympani, continued along the lateral aspect of the scala tympani, and terminated at millimeter 9.25, remaining entirely within the scala tympani (Figure 7). The tip of the electrode array was embedded in the spiral ligament and abutted the lateral cochlear wall (Figure 8). There was no disruption of the basilar membrane, organ of Corti, or stria vascularis, and no fracture of the osseous spiral lamina. A cellular immune response with multiple foreign body giant cells in the capsule of fibrous tissue that surrounded the electrode array was observed (Figure 8). The hook region and lower basal turn of the scala tympani were completely obstructed with a combination of loose fibrous tissue and new bone formation (Figure 7 and 8). Loose fibrous tissue extended 3.5mm apical to the tip of the electrode array track in the scala tympani (Figure 5D and 7). The scala vestibuli was also partially filled with loose fibrous tissue in the basal turn. Although there was new bone formation throughout the basal 9.25 millimeters of the cochlea, most of this new bone occurred within 2 mm of the cochleostomy in the scala tympani. The round window was almost completely obstructed with new intracochlear bone deposited along the medial aspect of the round window membrane. Figure 9A shows the small section of the round window that was not completely obstructed by bone. The scala tympani orifice of the cochlear aqueduct was obstructed by soft tissue and new bone deposition (Figure 9B).

## 4. Discussion

### 4.1 Human pathologic correlate of delayed hearing loss

Hearing preservation was initially achieved in this patient after implantation with the Iowa/Hybrid S8 cochlear implant, at a level that would have enabled use of both acoustic and electric hearing. Between 4 to 18 weeks post-implantation, however, his hearing preservation classification deteriorated from partial to minimal hearing preservation(Skarzynski et al. 2013), at which point acoustic hearing was non-functional. The pathologic findings in this case offer insight into possible mechanisms of delayed hearing loss in patients with initially preserved hearing after cochlear implantation.

This patient is representative of the typical electric acoustic stimulation candidate, with noise-induced and genetically predetermined sharply down-sloping sensorineural hearing loss. The pathologic correlate of his high frequency profound sensorineural hearing loss was complete absence of inner and outer hair cells in the basal half of the cochlea, and partial loss of spiral ganglion neurons throughout Rosenthal’s canal. This is consistent with the expected cochlear pathology in “sensory presbycusis”, as defined by Schuknecht and Gacek (Schuknecht & Gacek 1993).

Since this patient had symmetric pre-implantation hearing, the histologic findings in the unimplanted right ear are likely representative of the pre-implantation pathology in the left ear. At the time of death, seven years after implantation in the left ear, the inner hair cell, outer hair cell, and spiral ganglion neuron counts were essentially the same in both the implanted and unimplanted ears. Importantly, this demonstrates that long-term preservation of hair cell populations and spiral ganglion neurons after short electrode cochlear implantation is achievable. Preservation of hair cells, supporting cells, and spiral ganglion neurons is critical not only for hearing preservation in implant patients, but also for the application of future hearing loss treatments that may include molecular, genetic, or stem cell approaches.

In this patient, degeneration of the organ of Corti and/or SGNs does *not* account for the delayed loss of his residual low frequency hearing after cochlear implantation. This is consistent with animal models of delayed post-implantation hearing loss, which demonstrate no significant reductions in inner hair cell, outer hair cell, and spiral ganglion neuron counts as compared to animals with preserved hearing(Landry et al. 2011; Tanaka et al. 2014). Evaluation of the human temporal bone pathology confirms the validity of these animal models.

The notable pathologic correlate of delayed hearing loss in this patient was deposition of fibrous tissue and osteoid in the basal turn of the scala tympani and scala vestibuli. Significant fibrous tissue deposition and new bone formation after cochlear implantation in the guinea pig has been correlated with auditory brainstem response (ABR) threshold elevation(O”Leary et al. 2013); conversely, animals with stable preserved hearing have fibrous tissue occluding less than 10% of scala tympani in the basal turn only (Coco et al. 2007). A minor difference in the human pathology presented here, compared to the guinea pig model histology described by O’Leary et. al., is the apical extension of fibrous tissue significantly beyond the tip of electrode (as depicted in Figure 7) in this patient. Although the fibrous tissue extends nearly 4 millimeters apical to the electrode tip, it does not extend beyond the basal turn and thus does not directly account for the low frequency hearing loss. This implies that the delayed loss of low frequency hearing is related to either an alteration in cochlear mechanics, or a disturbance of the hair cell, afferent synapse, or spiral ganglion neuron physiology that is not seen at the light microscopic level.

The implanted ear also demonstrated endolymphatic hydrops in the ascending portion of the basal turn. Endolymphatic hydrops may occur after trauma (including surgery such as cochlear implantation or stapedectomy), after an inflammatory or infectious process, or idiopathically, as in Meniere’s Disease. In a human temporal bone pathology study, endolymphatic hydrops *within the cochlea* was invariably associated with sensorineural hearing loss (Merchant et al. 2005). However, sensorineural hearing loss in patients with Meniere’s Syndrome has not been correlated with the *degree* of hydrops or *intracochlear location* of hydrops. The finding of hydrops may be considered a histopathologic marker of intracochlear trauma or disruption of intracochlear homeostasis (Merchant et al. 2005), however, its direct role in the development of sensorineural hearing loss remains unknown.

### 4.2 Alteration in cochlear mechanics due to fibrous tissue deposition

Intracochlear deposition of fibrous tissue and osteoid occurs commonly after cochlear implantation (Li et al. 2007; Seyyedi & Nadol 2014), as it did in this case. It is reasonable to assume that scarring-induced mechanical changes can lead to a decrease in the intracochlear sound pressure differential required to drive neurosensory transduction. Three possible mechanisms are considered and discussed.

One possible mechanism is the increased impedance (decreased compliance) of the round window and occlusion of pressure outlets in scala tympani. Normally, air conduction relies on the standard two-window cochlear model: the cochlea has rigid walls with two compliant windows (oval and round windows) and is filled with a fixed volume of incompressible fluid. Other “windows” such as the vestibular and cochlear aqueducts do not contribute in air conduction because they have much higher impedances than the round window. Mechanical activity at the oval window coupled with the very compliant pressure-releasing round window allows for high scala vestibuli pressure and low scala tympani pressure. The large pressure differential created across the partition at the cochlear base is the cochlear pressure drive, which generates the traveling wave and initiates mechanosensory transduction for hearing (Figure 10A) (this concept, with accompanying pressure measurements, is explained in Stieger et al. 2013).

If the fibrous and bony tissue growth results in a significant increase in round-window impedance, as well as occlusion of other possible pressure-release outlets at the scala tympani side – such as the cochlear aqueduct – then pressures in both scalae would be similar and large. The pressure difference across the partition would then be small, resulting in the loss of input pressure drive. Tonndorf and Tabor demonstrated, however, that rigid fixation of the round window in live guinea pigs results in only 15 to 25 dB change in sensitivity via air conduction stimulation, compared to 35 to 60 dB change when the oval window is rigidly fixed (Tonndorf & Tabor 1962). Additionally, sealing the cochlear aqueduct resulted in an additional small threshold elevation in animals with round window fixation. Based on these animal data, soft tissue and bony obstruction of the round window and cochlear aqueduct seen in this case (Figure 10B) may account for part (~20 dB), but not all, of the patient’s delayed post-implantation hearing loss. It is important to note, however, that the cochlear aqueduct is patent in only 34% of normal human temporal bone specimens (Gopen Q. et al. 1997); this must be considered in the extrapolation of these animal experimental findings to the human.

A second possible mechanism is an increase in the impedance of the cochlear partition (including the basilar membrane) adjacent to the length of the short implant. This effect has been studied previously in two computational models of the passive mechanical properties of the cochlea – a finite element model (Kiefer et al. 2006) used to investigate increased stiffness and a lumped element model (Choi and Oghalai 2005) used to investigate increased damping. Both studies found that basilar membrane motion could be affected at the basal region where the partition impedances were increased, but not significantly in the apical region. Both studies concluded that increasing cochlear partition impedance in the basal region adjacent to the cochlear implant did not affect low-frequency apical hearing.

A third possible mechanism is increased impedance in scala tympani, and sometimes scala vestibuli as well. Choi and Oghalai (2005) used a lumped-element computational model to explore the effect of intracochlear fibrosis surrounding a short cochlear implant in scala tympani on residual hearing. They modeled the cochlea using a ladder network of lumped impedances, with series-path elements in scala vestibuli and scala tympani and shunt-path elements to capture the path across the partition. Intracochlear fibrosis was simulated by increasing the damping in the basal half of scala tympani, resulting in reduced basilar membrane velocity, with a bigger reduction at the apex of the cochlea than at the base. A simple interpretation is that the cochlear input pressure drive decreases as it travels along the cochlea from base to apex due to the increased damping along the basal half, and by the time it reaches the apex, the pressure is too low to stimulate the neurosensory cells. With this model, a factor of 100 increase in damping (a possibility) predicted approximately 20 dB elevation of low frequency thresholds, and a factor of 1000 increase in damping (less likely) predicted more than 60 dB elevation for low frequency thresholds. Additional fibrosis in scala vestibuli, which was also seen in this case (Figure 8A), could further decrease input pressure drive. Thus, increased scala tympani impedance due to intracochlear fibrosis of the basal half of the cochlea may lead to low-frequency hearing loss.

The round-window fixation and cochlear aqueduct occlusion experiments in the guinea pig, and the computational modeling data suggest that: (1) obstruction of the round window and cochlear aqueduct, and (2) increased scala tympani impedance due to intracochlear fibrosis should both produce significant hearing losses. In combination, this might account for the delayed post-implantation hearing loss observed in this patient. If this supposition is correct, optimization of surgical techniques and pharmacotherapies that reduce delayed intracochlear scarring may improve long term hearing preservation after cochlear implantation. To better understand air conduction with short cochlear implantation and subsequent delayed scarring, direct measurements of intracochlear pressures in fresh cadaveric temporal bones with cochlear implant and simulated scarring under controlled circumstances would be valuable.

## 5. Conclusion

No significant change in hair cell and spiral ganglion neuron counts, as compared to the contralateral temporal bone, was found on histologic evaluation of this human temporal bone after implantation with a short electrode cochlear implant. The patient had delayed hearing loss after implantation which may be explained, in part, by alterations in cochlear mechanics due to intracochlear scarring. There may be other mechanisms of delayed hearing loss that occur concurrently, such as dysfunction of the hair cell, spiral ganglion neuron, or synaptic transmission, which should also be considered as possible etiologies.

## Acknowledgments

This work was supported by three grants from the National Institutes of Health: 5R01DC000152-33 (JBN), 1U24DC013983-01 (JBN), and 5P50DC000242-29 (BJG).

We would like to thank and acknowledge the patient and his family for participation in the National Temporal Bone Registry. We also thank and acknowledge Barbara Burgess, Diane Jones, Jennifer O'Malley, and Meng Yu Zhu for histologic preparation of the specimens, and Garyfallia Pagonis for assistance in preparing and drawing the figures. We thank Barbara Herrmann PhD for assistance in interpretation of the audiograms.

## Abbreviations

| | |
|---|---|
| **ABR** | Auditory Brainstem Response (ABR) |
| **SGN(s)** | spiral ganglion neuron(s) |
| **dB** | decibels |
| **Hz** | Hertz |
| **KHz** | kilohertz |
| **mm** | millimeters |

## References


Adunka OF, et al. Hearing preservation and speech perception outcomes with electric-acoustic stimulation after 12 months of listening experience. The Laryngoscope. 2013 pp.n/a–n/a.

Choi C-H, Oghalai JS. Predicting the effect of post-implant cochlear fibrosis on residual hearing. Hearing Research. 2005; 205(1–2):193–200. [PubMed: 15953528]

Chole RA, Hullar TE, Potts LG. Conductive component after cochlear implantation in patients with residual hearing conservation. American journal of audiology. 2014; 23(4):359–364. [PubMed: 25165991]

Coco A, et al. Does cochlear implantation and electrical stimulation affect residual hair cells and spiral ganglion neurons? Hearing Research. 2007; 225(1–2):60–70. [PubMed: 17258411]

Eshraghi AA, et al. Blocking c-Jun-N-terminal kinase signaling can prevent hearing loss induced by both electrode insertion trauma and neomycin ototoxicity. Hearing Research. 2007; 226(1–2):168–177. [PubMed: 17098385]

Gantz BJ, Turner C. Combining acoustic and electrical speech processing: Iowa/Nucleus hybrid implant. Acta Oto-Laryngologica. 2004; 124(4):344–347. [PubMed: 15224850]

Gantz BJ, et al. Hybrid 10 Clinical Trial. Audiology and Neurotology. 2009; 14(1):32–38. [PubMed: 19390173]

Gantz, BJ., et al. Multicenter Clinical Trial of the Nucleus® Hybrid™ S8 Cochlear Implant: Final Outcomes. 2015. Submitted (Laryngoscope)

Gifford RH, et al. Cochlear implantation with hearing preservation yields significant benefit for speech recognition in complex listening environments. Ear and hearing. 2013; 34(4):413–425. [PubMed: 23446225]

Gifford RH, et al. Localization and interaural time difference (ITD) thresholds for cochlear implant recipients with preserved acoustic hearing in the implanted ear. Hearing Research. 2014; 312:28–37. [PubMed: 24607490]

Golub JS, et al. Spectral and temporal measures in hybrid cochlear implant users: on the mechanism of electroacoustic hearing benefits. Otology & neurotology: official publication of the American Otological Society, American Neurotology Society [and] European Academy of Otology and Neurotology. 2012; 33(2):147–153.

Gopen Q, Rosowski JJ, Merchant SN. Anatomy of the normal human cochlear aqueduct with functional implications. Hear Res. 1997 May; 107(1–2):9–22. [PubMed: 9165342]

Gstoettner W, et al. A new electrode for residual hearing preservation in cochlear implantation: first clinical results. Acta Oto-Laryngologica. 2009; 129(4):372–379. [PubMed: 19140036]

Halpin, C. Chapter 11: Measuring Audiometric Outcomes. In: Shin, J.; Hartnick, C.; Randolph, G., editors. Evidence Based Otolaryngology. 2008. p. 229

Huarte RM, Roland JT Jr. Toward hearing preservation in cochlear implant surgery. Current Opinion in Otolaryngology & Head and Neck Surgery. 2014; 22(5):349–352. [PubMed: 25101938]

Kiefer J, et al. Combined electric and acoustic stimulation of the auditory system: results of a clinical study. Audiology and Neurotology. 2005; 10(3):134– 144. [PubMed: 15724084]

Kiefer J, Böhnke F, Adunka O, Arnold W. Representation of acoustic signals in the human cochlea in presence of a cochlear implant electrode. Hearing Research. 2006; 221:36–43. [PubMed: 16962268]

Kopelovich JC, Reiss LAJ, Etler CP, Xu L, Bertroche JT, Gantz BJ, Hansen MR. Hearing loss after activation of hearing preservation cochlear implants might be related to afferent cochlear innervation injury. Otology & Neurotology. 2015 in press.

Landry TG, et al. Spiral ganglion neuron survival and function in the deafened cochlea following chronic neurotrophic treatment. Hearing Research. 2011; 282(1–2):303–313. [PubMed: 21762764]

Lenarz T, et al. European multi-centre study of the Nucleus Hybrid L24 cochlear implant. International Journal of Audiology. 2013; 52(12):838–848. [PubMed: 23992489]

Li PMMC, et al. Analysis of intracochlear new bone and fibrous tissue formation in human subjects with cochlear implants. The Annals of otology, rhinology, and laryngology. 2007; 116(10):731–738.

Merchant SN, et al. Pathophysiology of Ménière's Syndrome: Are Symptoms Caused by Endolymphatic Hydrops? Otology & Neurotology. 2005; 26:74–81. [PubMed: 15699723]

Merchant, SN. Methods of Removal, Preparation and Study. In: Merchant, SN.; Nadol, JB., editors. Schuknecht's Pathology of the Ear. Shelton, CT: People's Medical Pub. House-USA Inc; 2010. p. 3Y51

Nadol JB, Eddington DK, Burgess BJ. Foreign body or hypersensitivity granuloma of the inner ear after cochlear implantation: one possible cause of a soft failure? Otology & neurotology: official publication of the American Otological Society, American Neurotology Society [and] European Academy of Otology and Neurotology. 2008; 29(8):1076–1084.

O'Leary SJ, et al. Relations between cochlear histopathology and hearing loss in experimental cochlear implantation. Hearing Research. 2013; 298(C):27–35. [PubMed: 23396095]

O'Malley JT, et al. Correlation between histologic and radiographic reconstruction of intracochlear electrode position in human temporal bones. Audiology & neurootology. 2014; 19(3):184–192.

Reiss LAJ, Turner CW, Karsten SA, Erenberg SR, Taylor J, Gantz BJ. Consonant recognition as a function of the number of stimulation channels in the Hybrid short-electrode cochlear implant. The Journal of the Acoustical Society of America. 2012a; 132(5):3406–12. [PubMed: 23145621]

Reiss LAJ, Turner CW, Karsten SA, Erenberg SR, Taylor J, Gantz BJ. Consonant recognition as a function of the number of stimulation channels in the Hybrid short-electrode cochlear implant. The Journal of the Acoustical Society of America. 2012b; 132(5):3406–12. [PubMed: 23145621]

Roland, JT., et al. United States Multicenter Clinical Trial of the Cochlear™ Nucleus® Hybrid™ Implant System. 2015. Submitted (Laryngoscope)

Schuknecht HF, Gacek MR. Cochlear pathology in presbycusis. The Annals of otology. 1993; 102(1 Pt 2):1–16.

Seyyedi M, Nadol JB. Intracochlear inflammatory response to cochlear implant electrodes in humans. Otology & neurotology: official publication of the American Otological Society, American Neurotology Society [and] European Academy of Otology and Neurotology. 2014; 35(9):1545–1551.

Skarzynski H, et al. Towards a consensus on a hearing preservation classi. Acta Oto-Laryngologica. 2013; 133(Suppl 564)(S564):000–000.

Stieger C, Rosowski JJ, Nakajima HH. Comparison of forward (ear-canal) and reverse (round-window) sound stimulation of the cochlea. Hearing Research. 2013; 301:105–14. [PubMed: 23159918]

Tanaka C, et al. Factors associated with hearing loss in a normal-hearing guinea pig model of hybrid cochlear implants. Hearing Research. 2014; 316(C):82– 93. [PubMed: 25128626]

Tonndorf J, Tabor JR. Closure of the cochlear windows: its effect upon air-and bone-conduction. The Annals of otology, rhinology, and laryngology. 1962; 71:5–29.

Turner CW, Reiss LAJ, Gantz BJ. Combined acoustic and electric hearing: Preserving residual acoustic hearing. Hearing Research. 2008; 242(1–2):164–171. [PubMed: 18164883]

Usami S-I, et al. Hearing preservation and clinical outcome of 32 consecutive electric acoustic stimulation (EAS) surgeries. Acta Oto-Laryngologica. 2014; 134(7):717–727. [PubMed: 24834939]

Van Abel KM, et al. Hearing preservation among patients undergoing cochlear implantation. Otology & neurotology: official publication of the American Otological Society, American Neurotology Society [and] European Academy of Otology and Neurotology. 2015; 36(3):416–421.

Woodson, EA., et al. Cochlear Implants and Hearing Preservation. Advances in Oto-Rhino-Laryngology. Basel: KARGER; 2009. The Hybrid Cochlear Implant: A Review; p. 125-134.

- Human temporal bone pathology from a Hybrid cochlear implant patient is presented.
- Months after implantation, his initially preserved residual hearing deteriorated.
- Hair cell and cochlear neuron loss did not account for the delayed deterioration.
- Intracochlear fibrosis and new bone formation was found in the implanted ear.
- Intracochlear scarring may partly explain delayed post-implantation hearing loss.

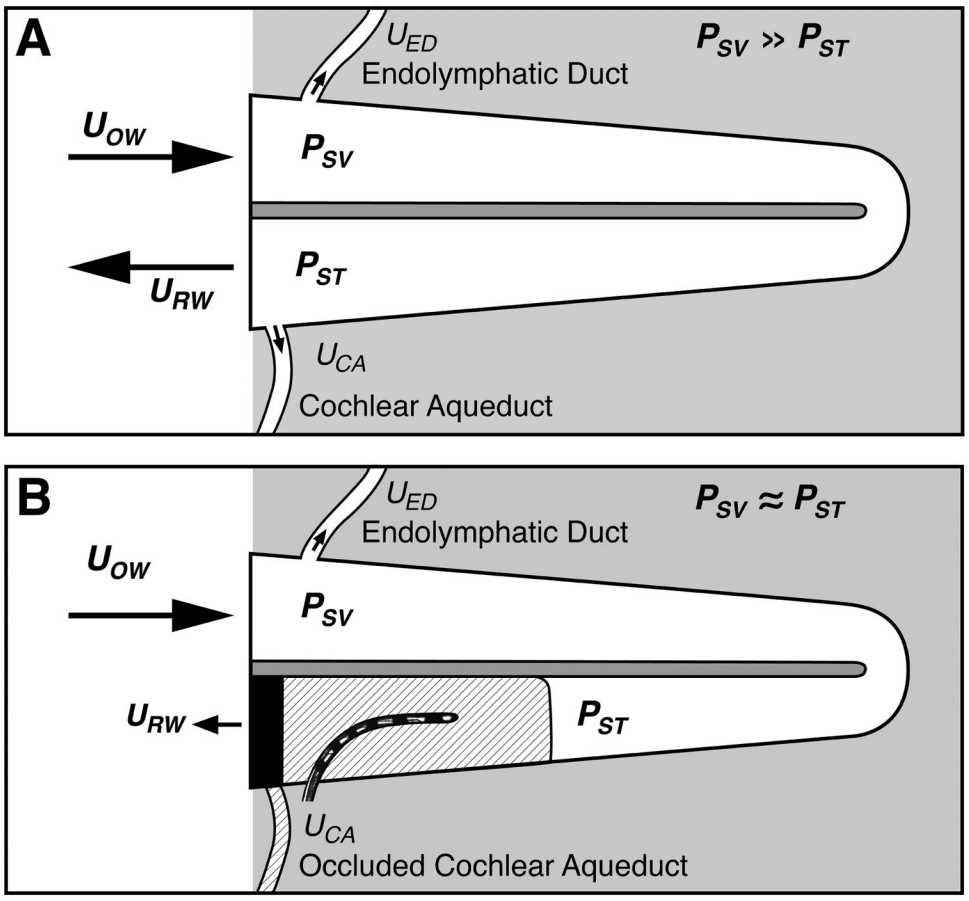


**Figure 1.**

Audiograms are labeled by weeks prior to or after cochlear implantation. Note the partial hearing preservation seen at 4 weeks after left sided implantation (B), and the profound left sensorineural hearing loss identified at 18 weeks after implantation (C). The left ear masked bone conduction thresholds in (B) and (C) most likely represent vibrotactile responses. The expected threshold for vibrotactile, rather than auditory, response at 250 Hz is 40 dB (Halpin 2008), and thus, this is in the range where vibrotactile responses are expected. The “?” symbols next to the left ear low frequency bone conduction thresholds indicate the audiologist’s note of suspected vibrotactile response. Therefore, there is no clear conductive component to the hearing loss.

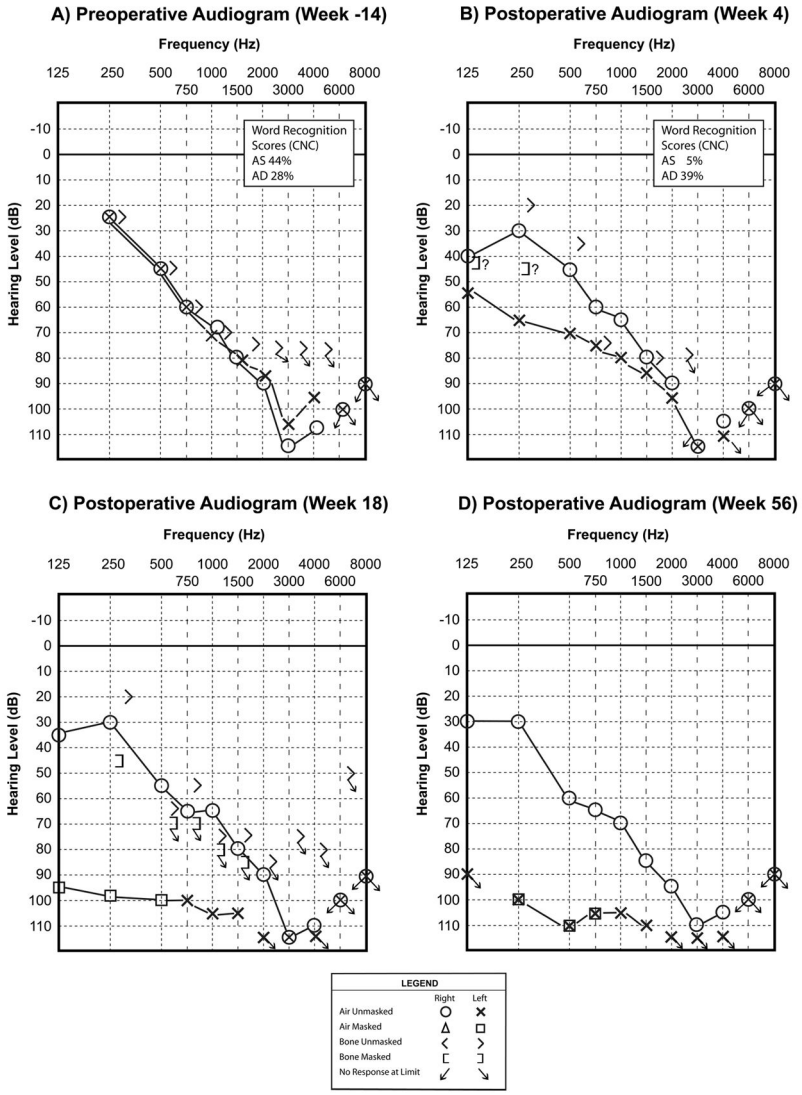


**Figure 2.**

(A) Photograph of the actual Iowa/Hybrid S8 electrode array removed from this patient's left temporal bone. (B) Schematic of intended intracochlear location for the Iowa/Hybrid S8 short electrode.

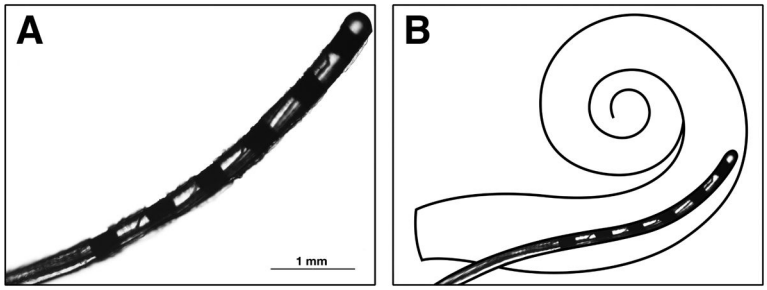


**Figure 3.**

(A) Current levels for this patient compared to other S8 and S12 Hybrid cochlear implant users measured one to three months after implantation, separated into those with stable hearing and those who developed hearing loss after activation. Red arrow indicates subject. The stable hearing group had less than 0.5 decibel per month increase in low frequency pure tone average (125, 250, 500, 1000 Hz), and the hearing loss group had greater than 30 decibel increase in low frequency pure tone average. Note that the approximate electrode position begins at 4 mm for S12 Hybrid patients and 6mm for S8 Hybrid patients. The shaded area indicates the range of programming levels for a group of Nucleus® Contour Advance™ implantees (Cochlear Ltd., Australia) for comparison.

(B) Electrode impedance measurements over time for this patient. Impedances obtained using the common ground electrode are shown for each of the 6 electrodes at the indicated time point relative to date of implantation (0 month).

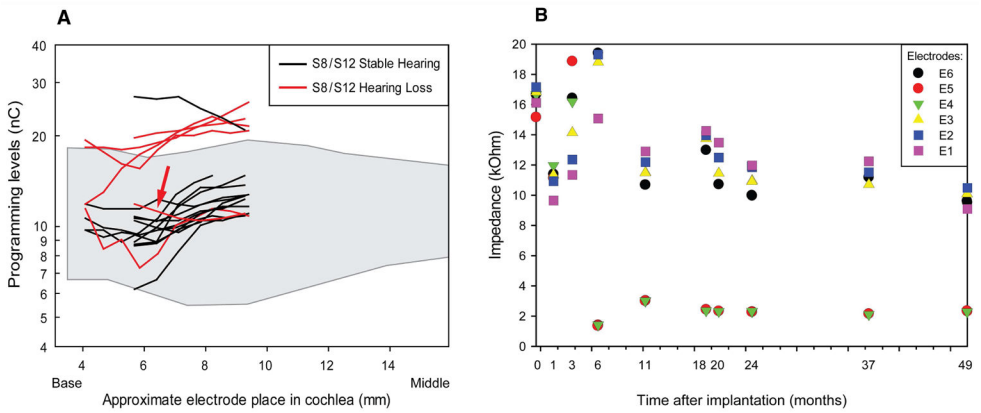


**Figure 4.**

Post-mortem computed tomography of left temporal bone specimen.

Arrow indicates the electrode array.

(A) The axial image shows the electrode in a lateral position in the lower basal turn.

(B) The Stenver's view image shows the intracochlear extension of the array with 6 hyperdensities representing the electrode contacts.

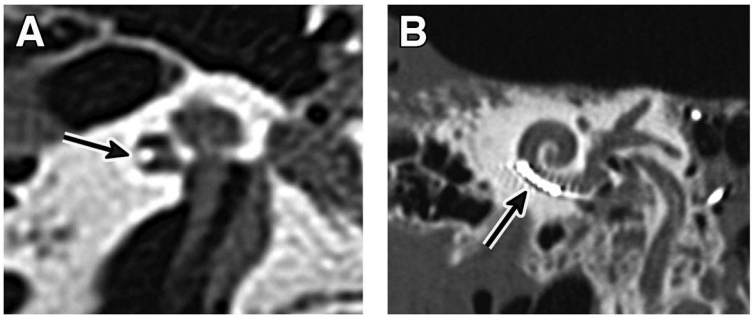


**Figure 5.**

Temporal bone sections, H&E stain. Middle turn, 20X, (A)right and (B) left both demonstrate similar preservation of organ of Corti cells, including some outer and inner hair cells. Basal turn, 20X, (C)right and (D)left both demonstrate total degeneration of the organ of Corti. Solid arrows indicate location or expected location of organ of Corti. In (D), which represents a section through the basal turn apical to the tip of the electrode array, (*) indicates loose fibrous tissue in scala tympani and open arrow indicates distension of Reissner's membrane.

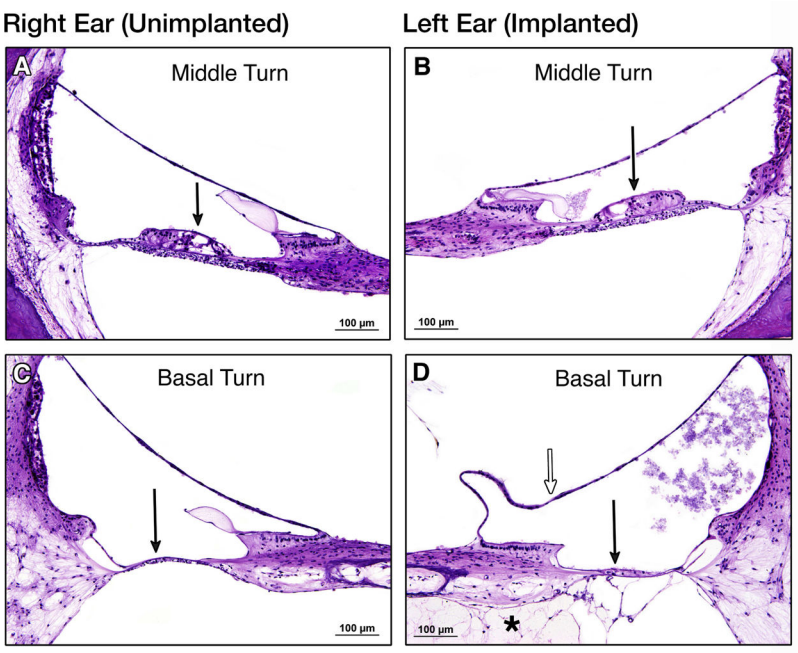


**Figure 6.**

Cytocochleogram for this patient. This represents the quantification of inner hair cells, outer hair cells, and spiral ganglion neurons (by cell body count) along the entire length of both right and left cochleae. The black areas represent absent hair cells or percent (%) loss of spiral ganglion neurons compared to an age-matched reference population (Merchant SN 2010). On the x-axis at the top, the location along the length of the cochlea is marked from apex to base, and the corresponding frequency map is shown. The location of the intracochlear electrode array is shown. There was essentially symmetric right ear (unimplanted) and left ear (implanted) inner hair cell, outer hair cell, and spiral ganglion neuron counts in this patient. mm= millimeters; Hz= Hertz

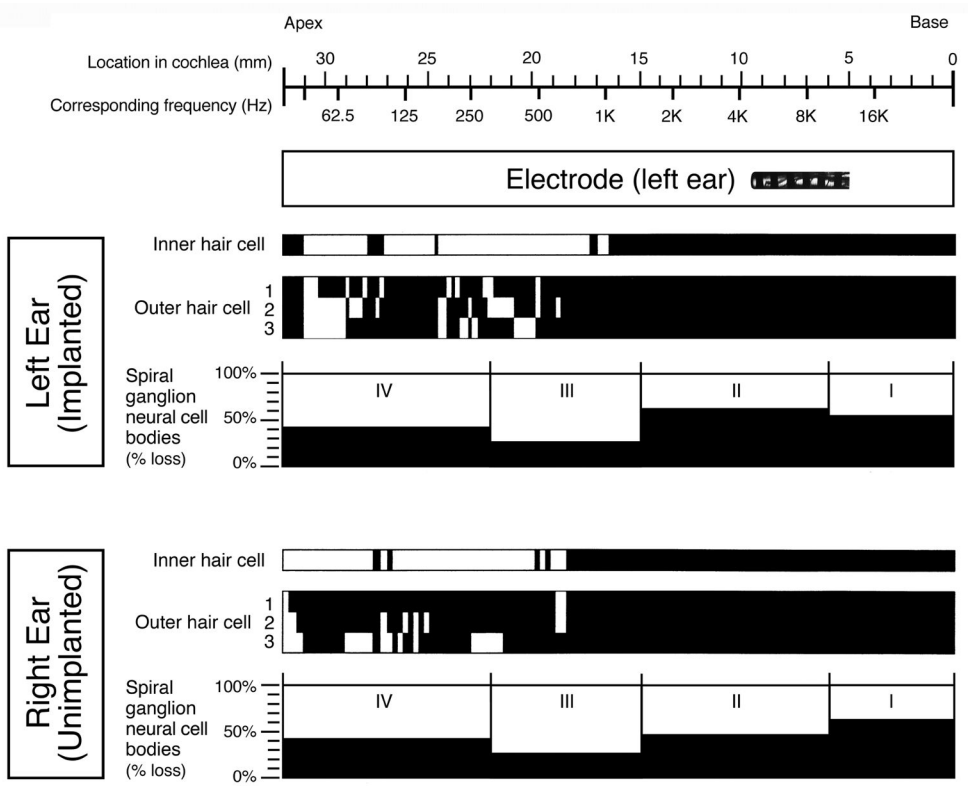


**Figure 7.**

Two dimensional cochlear reconstruction demonstrating the intracochlear electrode location and the location of fibrous tissue and bone deposition. Note that the electrode array was within the scala tympani, but new bone growth and fibrous tissue marked on the reconstruction was in the scala tympani and/or scala vestibuli. Slide section numbers are on the y-axis. The numbers along the cochlear duct indicate millimeters from the basal end of the cochlea, with a total cochlear duct length of 33.3 millimeters.

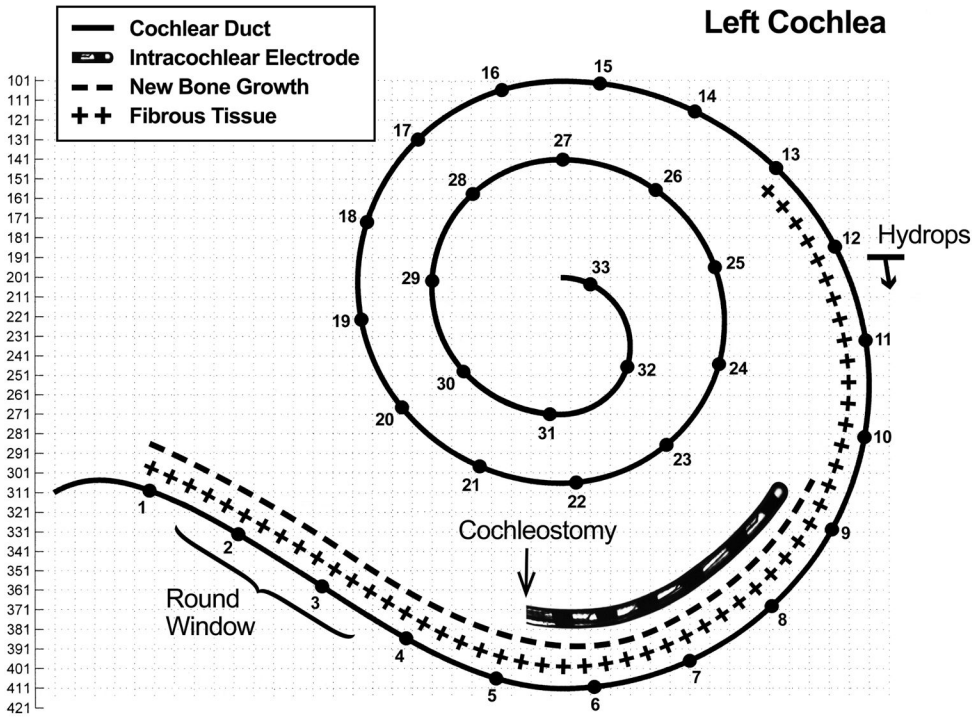


**Figure 8.**

Temporal bone sections, H&E stain. (*) indicates electrode array track in all images. (A) Low power section through basal turn demonstrating fibrous tissue throughout the scala tympani (++) and scala vestibuli (+), and distension of Reissner's membrane (triangle). (B) High power magnification of the black box area in (A), showing the capsule that formed around the electrode array in the scala tympani. (C) Low power section at the level of the cochleostomy (yellow arrows), showing a fibrous tissue seal, and new intracochlear bone and fibrous tissue. (D) High power magnification of the black box area in (C) showing the capsule around the electrode track. Red arrow indicates a foreign body giant cell.

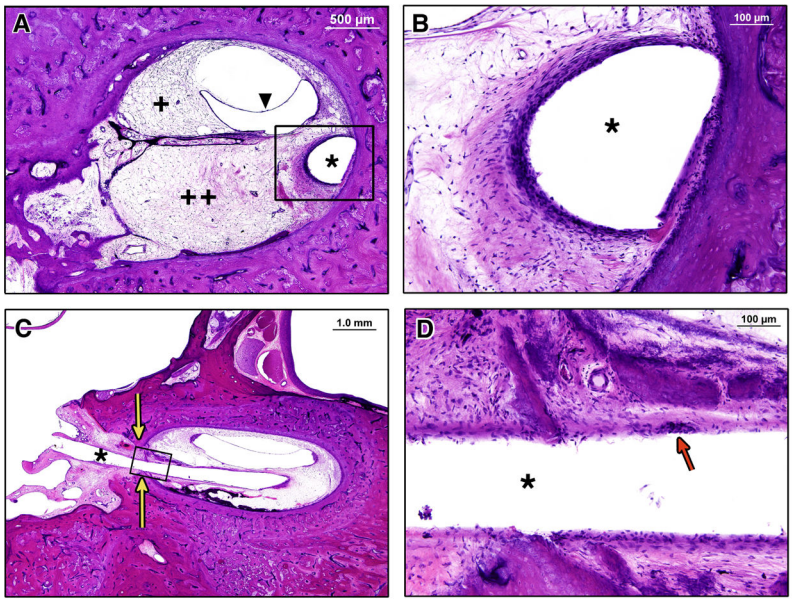


**Figure 9.**

Temporal bone sections, H&E stain. (A) Neo-ossification along the intracochlear aspect of the round window membrane and bony and fibrous obliteration of the basal end of the scala tympani. (B) Obstruction of the cochlear aqueduct by fibrous tissue and neo-ossification. RWN = round window niche. Arrows indicate neo-ossification. (+) indicates fibrous tissue.

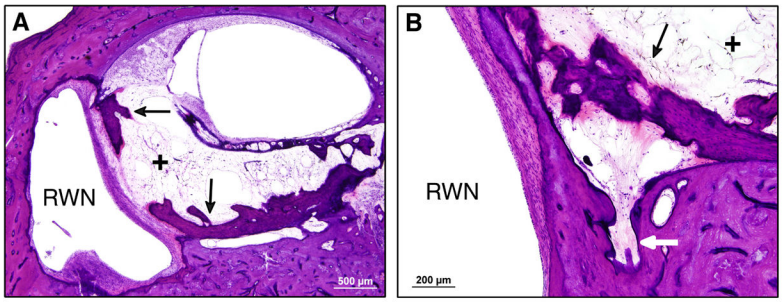


**Figure 10.**

Schematics of sound conduction through the cochlea and the effect of scar tissue in the basal turn of scala tympani. (A) A normal inner ear in which the low-impedance of the round window leads to equal but opposite volume displacements of the oval $\boldsymbol{U_{OW}}$ and round window $\boldsymbol{U_{RW}}$ (with insignificant volume displacement through the endolymphatic duct and cochlear aqueduct) when the oval window is driven by air-conducted sound. The difference in impedance at the windows also leads to a difference in the sound pressure between the scalae, where $\boldsymbol{P_{SV}}$ is the sound pressure in scala vestibule near the oval window, and $\boldsymbol{P_{ST}}$ is the sound pressure in scala tympani near the round window. The difference in scala sound pressure $\boldsymbol{P_{SV}}$ -$\boldsymbol{P_{ST}}$ is the pressure drive to the traveling wave and inner-ear sensory transduction. (B) The presence of bone and scar tissue in the basal scala tympani will reduce the volume displacement of the round window, equalize the scala pressures, reduce the difference in scala sound pressure, and reduce the pressure drive to the inner-ear. When the round window impedance is increased by the scarring, measureable volume velocity can occur through any open ‘third-windows’, e.g. the vestibular aqueduct (Tonndorf & Tabor 1962).

**Table 1**

Cochlear Implant Performance Assessment by CNC Word Recognition Scores (%)

| | Left Ear (CI or HA) | Right Ear (HA) | Both Ears (Bimodal)* |
|---|---|---|---|
| Pre-op | 24% (HA) | 40% | |
| 4 Months Post-op | | | 64% |
| 8 Months Post-op | | 32% | 60% |
| 3 Years Post-op | 16% (CI) | 31% | 68% |
| 4 Years Post-op | 28% (CI) | 37% | 73% |

*Bimodal: hearing aid in right ear and cochlear implant electric stimulation in left ear CI: cochlear implant, HA: hearing aid, Pre-op: preoperatively, Post-op: postoperatively

**Table 2**

Corrected Spiral Ganglion Neuron Count

| | Right Ear (Unimplanted) | Left Ear (Implanted) |
|---|---|---|
| Segment I | 1346 | 1661 |
| Segment II | 5182 | 4019 |
| Segment III | 4672 | 4651 |
| Segment IV | 4651 | 3992 |
| Total | 15,138 | 13,722 |
| Total compared to a normal count for age (%) | 56% | 51% |